

$\text{Ln}_2\text{Al}_3\text{Si}_2$ (Ln = Ho, Er, Tm): New Silicides from Molten Aluminum—Determination of the Al/Si Distribution with Neutron Crystallography and Metamagnetic Transitions**

Xian-Zhong Chen, Bradley Sieve, Robert Henning, Arthur J. Schultz, Paul Brazis, Carl R. Kannewurf, Jerry A. Cowen, Richard Crosby, and Mercouri G. Kanatzidis*

Silicides are both scientifically and technologically important, and have been extensively studied during the past several decades.^[1] Various topics and review articles can be found regarding their preparation, properties, crystal chemistry,^[2] thermodynamics,^[3] applications in silicon technology,^[4] and materials aspects for advanced technologies.^[5] Silicides are typically synthesized by direct reaction of the elements with heating to over 1000 °C and often with the necessary use of an arc-welder or induction furnace. Although single crystals can sometimes be obtained by annealing or quenching the product, in most situations only powder samples are formed with these traditional methods. This can complicate structure determinations and limit proper characterization. Recently, we have initiated exploratory synthetic investigations of silicides using metal fluxes and find that many new aluminum silicides form, most with novel structure types.^[6] These compounds usually decompose rapidly upon contact with acid, but they can be easily separated from the excess Al flux with aqueous sodium hydroxide solution. The products often consist of many single crystals with nice shapes. Here we present our results for the Ln/Al/Si systems (Ln = Ho, Er, Tm). There are few examples of rare earth aluminum silicides in the literature.^[7] Most of them were synthesized as powders, and their crystal structures have not been determined or refined. As for Ho, Er, and Tm, only $\text{Ln}_6\text{Al}_3\text{Si}$ (Ln = Ho, Tm)^[8] and Er_4AlSi_3 ^[9] have been described. Here we report on the new aluminum silicides $\text{Ln}_2\text{Al}_3\text{Si}_2$ (Ln = Ho, Er, Tm) synthesized in Al metal flux.

The black compounds $\text{Ln}_2\text{Al}_3\text{Si}_2$ ^[10] (Ln = Ho, Er, Tm) are stable in the air, water, and aqueous NaOH solution, but decompose instantaneously in aqueous HCl to release a gas which ignites upon contact with air. Mass spectrometry showed that the gas contains disilane (Si_2H_6) with a small amount of SiH_4 and there are no trisilanes or higher silanes detected. The lanthanides Ho, Er, and Tm behave differently from others in the series. For example La, Ce, Pr, Nd, and Sm give LnAlSi ,^[11] whereas La, Sm, Tb, and Yb give LnAl_2Si_2 .^[11] Neither of these two types of compounds has been found for Ho, Er, and Tm so far. Instead, the $\text{Ln}_2\text{Al}_3\text{Si}_2$ and LnAl_2Si ^[12] families seems to be more stable.

The three $\text{Ln}_2\text{Al}_3\text{Si}_2$ compounds are isostructural ($\text{Y}_2\text{Al}_3\text{Si}_2$ -type^[13]); they possess an $[\text{Al}_3\text{Si}_2]^{6-}$ framework filled with rare earth cations (Figure 1). The positions of Al and Si, which are

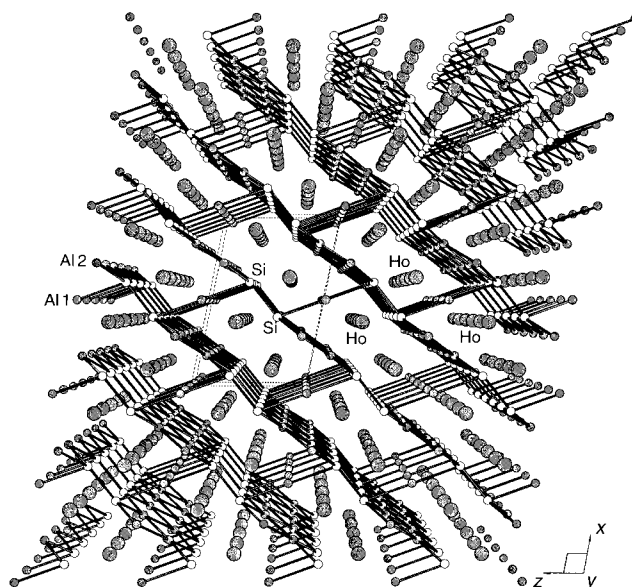


Figure 1. Perspective view of the structure of $\text{Ln}_2\text{Al}_3\text{Si}_2$ (Ln = Ho, Er, Tm).

almost impossible to determine on the basis of X-ray diffraction studies only, were decided on the basis of reasonableness of bond lengths around Al and Si. This choice was validated by the results of a neutron diffraction study (see below). In the $[\text{Al}_3\text{Si}_2]^{6-}$ framework, parallel Al–Al zigzag chains (by Al2) along the *b* direction are bridged by Si–Si dimers to form Al_2Si_2 layers perpendicular to the *ac* plane (Figure 2 A). The distances Al2–Al2, Al2–Si, and Si–Si are 2.768, 2.600, and 2.369 Å, respectively. Within the Al_2Si_2 layer, chairlike hexagonal rings that are formed by Si and Al2 atoms and edge-sharing along the *b* direction can also be seen. These layers are linked together by Al1 atoms, through linear Si–Al–Si bonds with a Si–Al distance of 2.721 Å, to form a three-dimensional structure. The structure shows parallel tunnels along the *b* direction, and two rows of rare earth atoms sit in each tunnel. Within each tunnel, the Ln–Ln distances are 4.027 (Ln = Ho), 4.018 (Ln = Er), and 4.005 Å (Ln = Tm), respectively, in each row and 3.765 (Ln = Ho), 3.754 (Ln = Er), and 3.749 Å (Ln = Tm), respectively, between the two rows. The shortest Ln–Ln distances, however, of 3.670, 3.648, and 3.628 Å for Ln = Ho, Er, and Tm, respectively, are found

- [*] Prof. Dr. M. G. Kanatzidis, Dr. X.-Z. Chen, B. Sieve
Department of Chemistry
Michigan State University
East Lansing, Michigan 48823 (USA)
Fax: (+1) 517-353-1793
E-mail: kanatzid@argus.cem.msu.edu
- R. Henning, Dr. A. J. Schultz
Argonne National Laboratory, IPNS, Bldg. 360
Argonne, IL 60439-4814
- P. Brazis, Prof. C. R. Kannewurf
Department of Electrical Engineering and Computer Science
Northwestern University, Evanston, IL 60208 (USA)
- Prof. J. A. Cowen, R. Crosby
Department of Physics and Center for Fundamental Materials Research
Michigan State University, East Lansing, MI 48824-1322
- [**] M.G.K. is a Camille and Henry Dreyfus Teacher Scholar 1993–1998. This work made use of the SEM facilities of the Center for Electron Optics at Michigan State University. Work at Argonne National Laboratory is sponsored by the Department of Energy, Office of Basic Energy Sciences (contract no. W-31-109-ENG-38).

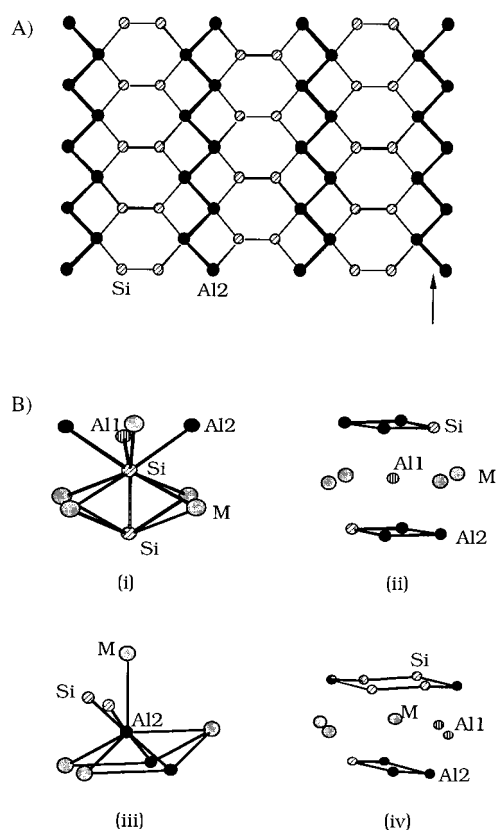


Figure 2. A) The structure of the Al_2Si_2 layer with atom labeling. The Al zigzag chains are marked with an arrow. B) The coordination environments of each atom in $\text{Ln}_2\text{Al}_3\text{Si}_2$ ($\text{Ln} = \text{Ho}, \text{Er}, \text{Tm}$).

between Ln atoms in adjacent tunnels and right above and below the Si–Si dimers. The presence of Si–Si dimers in the structure is consistent with mass spectrometry experiments which indicate the release of disilane upon treatment with acid. No trisilanes or higher silanes were detected. The coordination environments for different atoms are shown in Figure 2B.

To unequivocally determine the correct Al and Si positions in the structure, we performed a single-crystal neutron crystallographic analysis on $\text{Ho}_2\text{Al}_3\text{Si}_2$.^[14] The scattering neutron cross-sections of Al and Si differ by about 25%, which is enough to distinguish them from one another.^[15] Tables 1 and 2 show the atomic coordinates and selected bond distances obtained with this analysis, and they are in excellent agreement with those obtained from X-ray diffraction studies. This suggests that using expected bond lengths as a criterion for assigning Si and Al positions may be appropriate in most aluminum silicides, although the criterion will probably fail when high coordination numbers (>6) are involved.

The electrical conductivity and thermopower data on single crystals of the compounds indicate a p-type metallic behavior

Table 1. Atomic positions for $\text{Ho}_2\text{Al}_3\text{Si}_2$ as determined from the neutron diffraction data.

Atom	<i>x</i>	<i>y</i>	<i>z</i>	<i>U</i> / <i>U</i> _c × 100
Ho	0.61981(8)	0	0.32319(12)	0.46
Si	0.90690(16)	0	0.36033(23)	0.75
Al1	0	0	0	1.19
Al2	0.30502(21)	0	0.13414(29)	0.97

Table 2. Selected bond lengths [Å] for $\text{Ho}_2\text{Al}_3\text{Si}_2$ as determined from the neutron diffraction data.

Ho–Ho	3.6667(16)	Si–Si	2.3706(30)
Ho–Ho	3.7543(13)	Si–Al1	2.7129(15)
Ho–Si	2.8708(18)	Si–Al2	2.5983(15)
Ho–Si	2.9934(13)	Al1–Al2	3.0471(20)
Ho–Si	2.9459(12)	Al1–Al2	3.0646(15)
Ho–Al1	3.0117(7)	Al2–Al2	2.7688(25)
Ho–Al2	3.5077(20)		
Ho–Al2	3.1628(16)		

for all three compounds (see Figure 3 for data on $\text{Ho}_2\text{Al}_3\text{Si}_2$). The room-temperature conductivity of all compounds is very high at about $40\,000\text{ S cm}^{-1}$, while the corresponding thermopower is lower than $+3\text{ }\mu\text{V K}^{-1}$. Magnetic susceptibility data for $\text{Ho}_2\text{Al}_3\text{Si}_2$ are presented in Figure 4A. $\text{Tm}_2\text{Al}_3\text{Si}_2$ and $\text{Ho}_2\text{Al}_3\text{Si}_2$ show an antiferromagnetic (AF) transition with a

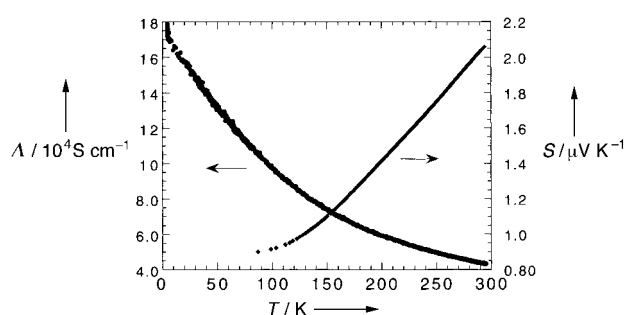


Figure 3. A) Temperature-dependent, four-probe electrical conductivity λ and thermopower data S for a single crystal of $\text{Ho}_2\text{Al}_3\text{Si}_2$.

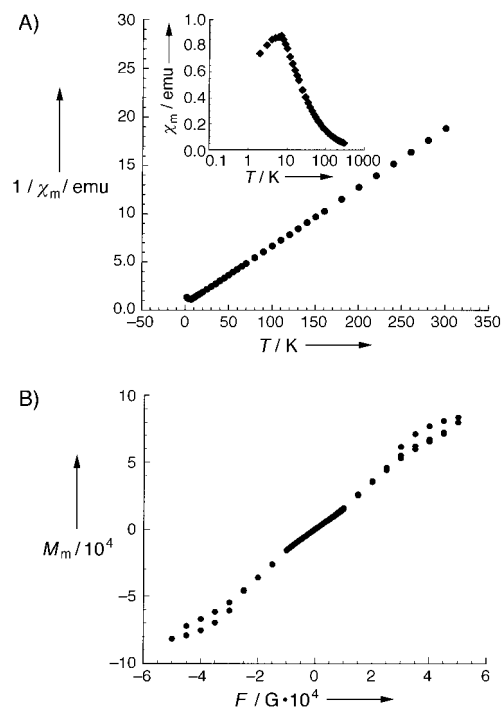


Figure 4. A) Plots of molar magnetic susceptibility χ_m [emu mol^{-1}] and $1/\chi_m$ [mol emu^{-1}] versus temperature [K] for $\text{Ho}_2\text{Al}_3\text{Si}_2$. Inset: an enlargement of the AF transition ($\lg T$ scale). B) Molar magnetization M_m of $\text{Ho}_2\text{Al}_3\text{Si}_2$ as a function of field strength F (hysteresis at 2.5 K). The magnetic susceptibilities were measured on ground crystals with a Quantum Design SQUID magnetometer between 2 and 300 K.

Néel temperature T_N of 7 K. Above this temperature, the data for both compounds follow the Curie–Weiss law, with Curie temperatures $\theta = -10.5$ and 4 K for $\text{Ho}_2\text{Al}_3\text{Si}_2$ and $\text{Tm}_2\text{Al}_3\text{Si}_2$, respectively. The AF transition for $\text{Er}_2\text{Al}_3\text{Si}_2$ occurs below 4 K. The measured effective magnetic moment at 300 K is $11.2 \mu_B$ for $\text{Ho}_2\text{Al}_3\text{Si}_2$ and $7.58 \mu_B$ for $\text{Tm}_2\text{Al}_3\text{Si}_2$; these values are close to the theoretical μ_{eff} for Ln^{3+} ($10.61 \mu_B$ for Ho^{3+} and $7.56 \mu_B$ for Tm^{3+}). Well below the AF transition temperature, the hysteresis, $M(H)$, curves taken on powder samples of the Tm and Ho compounds exhibit an inflection point at a critical field of about 6 kG with an increase in slope at higher fields. Such behavior is characteristic of the “spin-flop” transition in an antiferromagnet when the field is applied along the direction of sublattice magnetization. The magnetization of powder samples of the Ho compound has a similar inflection point at about 30 kG, which is characteristic of a metamagnetic transition. Data on single-crystal samples are necessary for the complete understanding of the magnetic properties of these isostructural compounds.^[16]

Three new rare earth aluminum silicides $\text{Ln}_2\text{Al}_3\text{Si}_2$ (Ln = Ho, Er, Tm) have been synthesized in molten Al.^[17] The Al flux acts as a good carrier for Si by solubilizing it and making it available for reaction, without forming a binary Al/Si compound. In the absence of Si, such reactions yield a variety of novel aluminides.^[18, 19] The compounds $\text{Ln}_2\text{Al}_3\text{Si}_2$ show an antiferromagnetic transition at low temperature and undergo “spin-flop” metamagnetic transitions upon the application of strong magnetic fields.

Experimental Section

Synthesis: In a N_2 -filled box, Ln metal (Ln = Ho, Er, Tm), Si, and Al were mixed in a vial in several different molar ratios with a large excess of Al and transferred into alumina containers, which were flame sealed in silica tubes under high vacuum. The samples were heated to 1000°C for 3 d, and then cooled to 300°C at -7.3°h^{-1} and finally to room temperature. The products were isolated as shiny black crystals after treatment with aqueous NaOH.

Single-crystal X-ray diffraction data were collected at room temperature with a Rigaku 4-circle diffractometer with $\text{MoK}\alpha$ radiation ($\lambda = 0.71073 \text{ \AA}$). Empirical absorption corrections, based upon ψ scans, were applied to the data. The structures were solved by direct methods. All calculations including structural refinements were performed by using the TEXSAN^[20] crystallographic software package. As in all Al- and Si-containing intermetallic compounds, Al and Si are difficult to distinguish. The current model gives the lowest R values, the best temperature factors, and a composition that is most consistent with the elemental analysis determined by energy-dispersive spectroscopy (EDS). As expected, the Ln–Si (Ln = Ho, Er, Tm) distances are shorter than the Ln–Al distances, and the Si–Al distances are longer than the Si–Si distance. More significantly, the bond distances clearly reveal the correct positions of the Al and Si atoms, and this is supported by the results of neutron diffraction experiments.

Received: March 2, 1998

Revised version: October 29, 1998 [Z11541 IE]

German version: *Angew. Chem.* **1999**, *111*, 695–698

Keywords: aluminum • conducting materials • lanthanides • magnetic properties • silicon

- [1] A. Szytuda, J. Leciejewicz in *CRC Handbook of Crystal Structures and Magnetic Properties of Rare Earth Intermetallics*, CRC Press, Boca Raton, FL, **1994**, p. 110, and references therein.
- [2] B. Aronsson, T. Lundström, S. Rundqvist in *Borides, Silicides and Phosphides*, Methuen, London, **1965**.

- [3] a) M. E. Schlesinger, *Chem. Rev.* **1990**, *90*, 607–628; b) T. G. Chart, *A Critical Assessment of Thermochemical Data for Transition Metal-Silicon Systems*, National Physical Laboratory, Teddington (UK), **1972** (NPL report on Chemistry 18).
- [4] A. H. Reader, A. H. Vanommen, P. J. W. Weijss, R. A. M. Wolters, D. J. Oostra, *Rep. Prog. Phys.* **1993**, *56*(11), 1397–1467.
- [5] K. Maex, *Appl. Surf. Sci.* **1991**, *53*, 328–337.
- [6] X. Z. Chen, S. Sportouch, B. Sieve, J. Cowen, C. R. Kannewurf, P. Brazis, M. G. Kanatzidis, *Chem. Mater.* **1998**, *10*, 3202–3211.
- [7] There exist several older reports on the production of binary compounds such as LnSi_2 , ThSi_2 , MoSi_2 , and WSi_2 with the use of molten aluminum. However, most of these materials are in fact metal aluminum silicides (e.g. LnAlSi) rather than metal silicides: X. Z. Chen, B. Sieve, M. Zhuravleva, P. Brazis, C. R. Kannewurf, M. G. Kanatzidis, unpublished results; a) O. Höningschmid, *Monatshefte Chemie* **1906**, *27*, 1069; b) G. Brauer, A. Mitius, *Z. Anorg. Allg. Chem.* **1942**, *249*, 325–339; c) G. Brauer, H. Haag, *Z. Anorg. Allg. Chem.* **1952**, *267*, 198–212.
- [8] I. S. Dubenko, A. A. Evdokimov, Yu. N. Titov, *Russ. J. Inorg. Chem. Engl. Transl.* **1985**, *30*(11), 1707–1708.
- [9] A. Raman, *Inorg. Chem.* **1968**, *7*, 973–976.
- [10] Single-crystal X-ray diffraction data were collected at room temperature with a Rigaku four-circle diffractometer with $\text{MoK}\alpha$ radiation ($\lambda = 0.71073 \text{ \AA}$). Crystal data for $\text{Ln}_2\text{Al}_3\text{Si}_2$ (Ln = Ho, Er, Tm): crystal sizes $0.10 \times 0.07 \times 0.35$ (Ln = Ho), $0.14 \times 0.08 \times 0.40$ (Ln = Er), $0.10 \times 0.06 \times 0.10$ (Ln = Tm); $a = 10.126(1)$, $b = 4.0266(9)$, $c = 6.5812(8) \text{ \AA}$, $\beta = 100.93(1)^\circ$, $V = 263.48(7) \text{ \AA}^3$ (Ln = Ho); $a = 10.083(3)$, $b = 4.0175(9)$, $c = 6.566(1) \text{ \AA}$, $\beta = 100.73(2)^\circ$, $V = 261.3(1) \text{ \AA}^3$ (Ln = Er); $a = 10.043(2)$, $b = 4.0050(8)$, $c = 6.550(3) \text{ \AA}$, $\beta = 100.54(3)^\circ$, $V = 259.0(1) \text{ \AA}^3$ (Ln = Tm); space group $C2/m$, $Z = 2$; $\mu = 30.968$ (Ln = Ho), 33.127 (Ln = Er), 35.204 mm^{-1} (Ln = Tm); total reflections: 1408 (Ln = Ho), 1754 (Ln = Er), 1720 (Ln = Tm); unique: 343 [$R(\text{int}) = 0.036$, Ln = Ho], 434 [$R(\text{int}) = 0.033$, Ln = Er], 430 [$R(\text{int}) = 0.077$, Ln = Tm]; observed ($I > 3\sigma$): 338 (Ln = Ho), 429 (Ln = Er), 418 (Ln = Tm); index ranges $-13 \leq h \leq 13$, $-5 \leq k \leq 5$, $-9 \leq l \leq 9$ (Ln = Ho), $-14 \leq h \leq 14$, $-6 \leq k \leq 6$, $-9 \leq l \leq 9$ (Ln = Er), $-14 \leq h \leq 14$, $-6 \leq k \leq 6$, $-9 \leq l \leq 9$ (Ln = Tm); $R/wR(I > 3\sigma)$ and GOF: 0.039/0.043 and 2.76 (Ln = Ho), 0.027/0.034 and 2.10 (Ln = Er), 0.026/0.032 and 1.43 (Ln = Tm), where $R = \Sigma ||F_o| - |F_c|| / \Sigma |F_o|$ and $wR = [(\Sigma w(|F_o| - |F_c|)^2) / \Sigma wF_o^2]^{1/2}$.
- [11] X. Z. Chen, M. Zhuravleva, P. Small, C. R. Kannewurf, P. Brazis, J. A. Cowen, R. Crosby, M. G. Kanatzidis, unpublished results.
- [12] P. Small, M. Zhuravleva, B. Sieve, M. G. Kanatzidis, unpublished results.
- [13] T. I. Yanson, M. B. Manyakov, O. I. Bodak, R. E. Gladyshevskii, R. Cerny, K. Yvon, *Acta Crystallogr. Sect. C* **1994**, *50*, 1377.
- [14] A single crystal ($1 \times 1 \times 2 \text{ mm}^3$) of $\text{Ho}_2\text{Al}_3\text{Si}_2$ was mounted on an aluminum pin and placed on the SCD diffractometer at the Intense Pulsed Neutron Source (IPNS) at Argonne National Laboratory. A position-sensitive area detector was used to obtain time-of-flight Laue data with a wavelength range of $0.7 - 4.2 \text{ \AA}$ for 25 settings of the crystal to cover two octants of reciprocal space. The details of the data collection and analysis procedures have been described previously.^[14a] A wavelength-dependent spherical absorption correction was applied.^[14b] Since extinction is strongly dependent on wavelength, symmetry-related reflections were not averaged. The structural refinement was performed using the GSAS program.^[14c] Since the ordering of the aluminum and silicon atoms needed to be determined, several models were refined with the anions in various positions. The lowest R value was obtained with the original model (determined from bond distance arguments), while the R value was at least 1.5% higher when the anions were switched. The anisotropic thermal parameters also suggested that the original model was correct. The fractional occupancies of the aluminum and silicon positions were also refined in each model to see if any mixing occurs on the sites. The occupancies of the aluminum and silicon in the original model obtained from X-ray diffraction refined to unity within 3σ , while the occupancies in the other models refined to 0.18(1) with aluminum on a silicon site and 0.82(1) with silicon on an aluminum site. These values are consistent with fully occupied silicon and aluminum positions. The neutron data confirm that the X-ray diffraction model is correct and that no disorder occurs between the aluminum and silicon positions.

- a) A. J. Schultz, K. Srinivasan, R. G. Teller, J. M. Williams, C. M. Lukehart, *J. Am. Chem. Soc.* **1984**, *106*, 999; b) R. A. J. Jacobson, *Appl. Crystallogr.* **1986**, *19*, 283; c) A. C. Larson, R. B. Von Dreele, *GSAS-General Structure Analysis System*, Los Alamos National Laboratory, **1994**.
- [15] Radiation: neutrons, $\lambda = 0.7\text{--}4.2\text{ \AA}$; data collection by the time-of-flight Laue technique with a position-sensitive area detector; $i(\theta)$ [cm^{-1}] = $0.195 + 0.550\theta$; extinction parameter g [rad^{-1}] = $2.1(1) \times 10^{-5}$; number of reflections in the final least-squares refinement with $F_o^2 > 3\sigma(F_o^2)$ 841; number of unique reflections 728; variables 48; minimized function $\sum w(F_o - F_c)^2$; $R_w(F_o^2) = 0.110$, $R(F^2) = 0.112$, $R_w(F) = 0.054$, $R(F) = 0.064$, GOF = 5.87.
- [16] B. Sieve, J. A. Cowen, M. G. Kanatzidis, unpublished results.
- [17] Recently we discovered that $\text{Dy}_2\text{Al}_3\text{Si}_2$ is isostructural to the compounds reported here, and it too exhibits a metamagnetic transition.
- [18] a) S. Niemann, W. Jeitschko, *J. Solid State Chem.* **1995**, *114*, 337–341; b) S. Niemann, W. Jeitschko, *Z. Kristallogr.* **1995**, *210*, 338–341; c) S. Niemann, W. Jeitschko, *J. Solid State Chem.* **1995**, *116*, 131–135; d) S. Niemann, W. Jeitschko, *J. Alloys Compd.* **1995**, *221*, 235–239.
- [19] P. C. Canfield, Z. Fisk, *Philos. Mag. B* **1992**, *65*, 1117–1123.
- [20] "TEXSAN—TEXRAY Structure Analysis Package", Molecular Structure Corporation, The Woodlands, TX, **1992**.

Functional Molecular Thin Films: Topological Templates for the Chemoselective Ligation of Antigenic Peptides to Self-Assembled Monolayers**

Lukas Scheibler, Pascal Dumy, Mila Boncheva, Kirsten Leufgen, Hans-Jörg Mathieu, Manfred Mutter, and Horst Vogel*

The study of molecular thin films for use in the controlled design of interfacial properties^[1] that have important implications in many different fields ranging from research on friction, lubrication and wetting,^[2] development of micro- and nanoscale devices^[3] to biocompatible surfaces, has attracted considerable interest.^[4] Most of the work has concentrated on

self-assembled monolayers (SAMs), in particular on the self-assembly of sulfur-bearing molecules such as thioalkanes^[5] and lipids^[6] on the surface of gold, or suitable silanes to hydroxylated surfaces (usually silicon oxide or glass).^[7] Self-assembled molecular thin films that comprise biopolymers are most interesting for the development of novel analytical techniques.^[8] Several novel micropatterning techniques have opened the possibility for the creation of multiarray sensor devices on the level of SAMs.^[9] In particular in the latter case, a generally applicable method for the design and synthesis of complex functional peptides suitable for the integration into SAMs is still a demanding task. We have shown recently that tethering template-assembled synthetic proteins (TASP) that expose metal or antigenic binding sites to SAMs results in highly sensitive and selective functional surfaces.^[10, 11] Here we elaborate novel strategies based on the template concept for the regioselective functionalization of SAMs on gold surfaces. In particular, regioselectively addressable functional templates (RAFT) that feature differentially reactive, spatially distinguishable domains in combination with chemoselective ligation procedures are used for the covalent attachment of antigenic peptides to SAMs. The formation of the SAM, its functionalization by several consecutive surface chemistry reactions, and the final binding of antibodies to the tethered TASP, were monitored and controlled by surface plasmon resonance (SPR), time-of-flight secondary-ion mass spectrometry (TOF-SIMS), and Fourier transform infrared (FTIR) spectroscopy. These methods are capable of measuring molecular reactions on gold surfaces: SPR delivers direct and continuous information on the mean concentration of the molecules on the surface during the formation of monomolecular films, TOF-SIMS allows the direct analysis of the chemical composition of SAMs, FTIR spectra carry information on both the presence of specific functional groups and the conformation of the molecules on the gold surface. The FTIR spectra were obtained by a recently developed attenuated total reflection (ATR) technique where the ATR crystal was covered by a gold film that is thin enough to be transparent for the infrared light but thick enough to serve as a continuous gold surface for the formation of SAMs by thioalkanes.^[12]

As a representative example of this general approach of functionalizing SAMs we covalently coupled a derivative of the antigenic (NANP)₃ peptide to a SAM of topological templates. This peptide was chosen because of its relevance to the immune response against malaria parasites; in another context it has been immobilised on gold surfaces by thioalkane linkers.^[13] As the RAFT molecule we used a cyclic peptide of the sequence $c[(\text{K}(\text{Boc})\text{K}(\text{Boc})\text{PGK}(\text{Alloc}))_2]$ **1**, which features orthogonally protected attachment sites on opposite faces of the cycle.^[14] Carboxythioalkanes were attached in bulk solution to the lower face of the deprotected K(Alloc) side chains of the template **1**, followed by the coupling of serines to the remaining deprotected K(Boc) sites of the serine groups. Subsequently, the RAFT molecule **2** was self-assembled on a gold surface through the thioalkane linkers. The hydroxyl groups on the four serine side chains that are on the upper face of the template were oxidized to aldehyde functions (Figure 1). Finally, the aminooxyacetyl-containing antigenic peptide **4** was ligated to the surface-

[*] Prof. H. Vogel, Dr. M. Boncheva,^[+] Dr. K. Leufgen
LCPPM, Institute of Physical Chemistry
Swiss Federal Institute of Technology Lausanne (EPFL)
CH-1015 Lausanne (Switzerland)
Fax: (+41)21-693-6190
E-mail: horst.vogel@epfl.ch

Prof. M. Mutter, Dr. L. Scheibler,^[++] Prof. P. Dumy^[+++]
Institute of Organic Chemistry, University of Lausanne
(Switzerland)

Prof. H.-J. Mathieu
LMCH, Institute of Material Sciences, EPFL (Switzerland)

[+] Current address:
Chalmers University of Technology
Department of Physical Chemistry, Göteborg (Sweden)

[++] Current address:
Harvard Institute of Medicine
Division of Bone and Mineral Metabolism, Boston (USA)

[+++] Current address:
LEDSS, Université J. Fourier, Grenoble, (France)

[**] This work was financially supported by the Board of the Swiss Federal Institutes of Technology (MINAST: 7.06).